
Current Methods for Drug Property Prediction in the Real World

Jacob Green
DeepMirror
jacob@deepmirror.ai

Cecilia Cabrera Diaz
DeepMirror
cecilia@deepmirror.ai

Maximilian A. H. Jakobs
DeepMirror
max@deepmirror.ai

Andrea Dimitracopoulos
DeepMirror
andrea@deepmirror.ai

Mark van der Wilk*
Imperial College London
m.vdwilk@imperial.ac.uk

Ryan D. Greenhalgh†
DeepMirror
ryan@deepmirror.ai

Abstract

Predicting drug properties is key in drug discovery to enable de-risking of assets before expensive clinical trials, and to find highly active compounds faster. Interest from the Machine Learning community has led to the release of a variety of benchmark datasets and proposed methods. However, it remains unclear for practitioners which method or approach is most suitable, as different papers benchmark on different datasets and methods, leading to varying conclusions that are not easily compared. Our large-scale empirical study links together numerous earlier works on different datasets and methods; thus offering a comprehensive overview of the existing property classes, datasets, and their interactions with different methods. We emphasise the importance of uncertainty quantification and the time and therefore cost of applying these methods in the drug development decision-making cycle. We discover that the best method depends on the dataset, and that engineered features with classical ML methods often outperform deep learning. Specifically, QSAR datasets are typically best analysed with classical methods such as Gaussian Processes while ADMET datasets are sometimes better described by Trees or Deep Learning methods such as Graph Neural Networks or language models. Our work highlights that practitioners do not yet have a straightforward, black-box procedure to rely on, and sets the precedent for creating practitioner-relevant benchmarks. Deep learning approaches must be proven on these benchmarks to become the practical method of choice in drug property prediction.

1 Introduction

In the high-stakes field of drug discovery, where the development of a new pharmaceutical often takes 10 to 15 years and requires investment exceeding \$1bn before it is available to the public, the need for more efficient strategies is apparent. Predictive models are emerging as a compelling solution for the virtual screening of compounds, which can reduce the need for costly synthesis or execution of expensive assays during the hit-to-lead or lead optimisation phases of drug discovery, by helping focus experiments on compounds likely to be effective, based on previously gathered data.

To discover such new compounds, one has to both exploit known effective structures and explore ones further afield from previously measured ones [13]. Therefore, practitioners need to both predict properties and quantify prediction uncertainty to identify structures that have good properties with

*Work done while at DeepMirror.

†Corresponding author.

low uncertainty (exploit) and those that have high uncertainty but potentially even better properties (explore). Robust uncertainty quantification provides a more nuanced understanding of prediction outcomes, allowing practitioners to integrate these predictions seamlessly into other decision-making frameworks. Therefore, the development and application of effective uncertainty quantification methods can significantly enhance the efficiency and cost-effectiveness of the drug discovery process.

Traditional methodologies such as Random Forests (RF) and Support Vector Machines (SVM) have demonstrated efficacy in molecular property prediction [33, 37, 29, 40, 32], but the relative performance of a specific method compared to the others varies across datasets. The development of deep learning, specifically Graph Neural Networks (GNNs), has further complicated choosing the best method [36, 35, 43]. While GNNs show potential, their performance gain is inconclusive when compared across various studies and compared to classical models [33, 18]. Pre-training techniques using GNNs [31, 14], language models, [41, 5], and 3D structures [30] have shown promise, but have not been sufficiently benchmarked against competing methods to draw conclusions about general performance. So, in spite of the development of many methods, there has never been a comprehensive comparison, and it is therefore difficult to make a fully informed decision when selecting the most appropriate machine learning model for molecular property prediction. Additionally, these methods rarely quantify uncertainty leading to a significant gap in the literature. Our work aims to address this gap and navigate these inconsistencies, thereby providing a more comprehensive understanding of selecting the optimal method for molecular property prediction with uncertainty quantification. Hence, we endeavour to answer the following research questions:

- RQ1.** From a large collection of classical methods (GPs, SVMs, RFs etc.) and modern methods (GNNs and language models), does one consistently outperform across a variety of datasets?
- RQ2.** Can groups of datasets be identified where a specific method routinely outperforms all others?
- RQ3.** How can one quantify and validate the uncertainty of different methods?
- RQ4.** What are the trade-offs between computational time and predictive performance in the application of these methods?

Answering these questions provides actionable advice to practitioners aiming to build predictive models for molecular datasets. In addition, it provides a clear assessment of how modern deep learning techniques compare to classical methods for these problems, and sets a standard that needs to be reached for a method to become a clear method of choice.

2 Problem Setting: Drug Property Prediction and Datasets

During drug development, two classes of properties are generally predicted: Absorption, Distribution, Metabolism, Excretion, and Toxicity (ADME(T)) and Quantitative Structure-Activity Relationships (QSAR). ADME(T) properties are often optimised to fall within a given range in order for them to be safe and effective for patients. QSAR refer to properties that are drug specific, such as the inhibitory effect on a target enzyme, or the binding affinity to a particular receptor that is linked to a disease. Being able to accurately predict these properties prior to carrying out laboratory testing is crucial to reduce the time and resources needed to bring safe and effective new drugs to patients. There are several public repositories with datasets of ADME(T) and QSAR properties that can be used for developing and benchmarking predictive models, the most prominent of which are the Therapeutics Data Commons (TDC) [15, 16], MoleculeNet [36], and OPERA [23].

Overall, the existing literature presents an incomplete, or even conflicting picture of the performance of GNNs and classical ML methods in drug property regression problems, as most earlier works test against a single benchmark and only with subsets of machine learning methods (section 3.2). While this can be expected to an extent given practical constraints on running evaluations, it complicates selecting a model for practitioners in science and business, who need an effective solution for their application. We believe that providing results on MoleculeNet is not sufficient to provide an idea of performance across drug property prediction classes. Many other papers only compare subsets of classical methods, leaving out some candidates (such as Gaussian Processes) altogether. Uncertainty in predictions is a vital element in de-risking decision making during drug discovery, yet only a small subset of research studies have been conducted to evaluate uncertainty [8, 43, 12].

We aim to address these gaps by comparing a wide set of methods, over a wide range of datasets, while also evaluating uncertainty quantification, to gain the first complete picture of how such problems can be tackled at scale. We select as wide a range of datasets as possible, but restrict ourselves to regression datasets, as they are more meaningful and realistic in real-world settings because:

1. Most molecular property prediction classification tasks are derived by thresholding regression problems, resulting in loss of information.
2. When converting a problem into a classification task, practitioners must choose a subjective threshold which may differ among individuals, even within the same organisation. This also influences performance metrics and model considerations (e.g. through class imbalance).

In addition, we take care to include difficult datasets with “activity cliffs”, where minor alterations in molecular structure can cause significant property changes (by several orders of magnitude). We obtain these from the curated ChEMBL datasets from MoleculeACE [33].

For all benchmark datasets [33, 36, 15, 23], we adhered to the default split as reported in the original benchmark. For the remaining datasets, we conducted train/test splits using a MaxMin splitter [26] to ensure that compounds in the test set were structurally dissimilar from those in the training set. In total, we benchmarked 184 machine learning methods on 44 regression datasets, covering two parent property classes: QSAR (32) and ADME(T) (12). See Table A.1 for a detailed overview.

3 Current Methods and Challenges in Drug Property Prediction

3.1 Method Overview

Input generation A common representation of molecules is the Simplified Molecular Input Line Entry System (SMILES), a compact notation that uses ASCII strings to represent chemical structures in a readable format. All benchmark datasets describe individual molecules using SMILES. In order to construct predictive models for molecular structures, these structures must first be translated into a numerical form, with three of the most popular approaches being:

1. **Cheminformatics molecular descriptors** that are designed using human understanding. These are constructed based on an extensive range of precalculated properties, encompassing geometrical, electronic, and thermodynamic attributes. Some techniques stop here, while others examine each atom in the molecule and its local environment up to a defined radius or bond distance, then formulate a unique identifier (fingerprint bit) for each atom and its corresponding environment, typically via a hashing procedure.
2. **Graph representations** where atoms are depicted as nodes and bonds as edges. The encoding of atoms and bonds within nodes and edges can be achieved in various ways, such as one-hot encodings or vectors characterised by physical properties. With graph representations, it is possible to apply graph-based machine learning algorithms to predict properties of the molecule directly from its structure.
3. **Tokenisation** of SMILES strings, by segmenting the string into smaller chunks or tokens, which typically involves breaking down the string into individual atoms, bonds, and ring closures. Tokenised SMILES can be inputs to language models, e.g. Transformers.

Classical vs. Deep Learning Different machine learning models can work with different input formats. In this paper, we distinguish “classical” machine learning methods, and deep learning methods. Classical methods require inputs to be real-valued vectors, and do little in the form of automatic feature design or extraction. As such, they are highly reliant on descriptive features being designed *before* being passed to the machine learning method. Deep learning, on the other hand, operates on representations of the data that are less pre-processed, like the graph representation or tokens, which allows feature representations to be learned in a data-driven manner, thus overcoming the limitations of fixed features. Specialised architectures have been developed to deal with graph or sequence structured inputs (GNNs [43] and Transformers [5, 41, 4]). Deep learning can also be applied to extract features, which can then be used as inputs to classical methods, as explained below.

Classical methods The fixed features that classical methods rely on can be human-designed, or learned in a self-supervised or unsupervised manner using deep learning. Features learned from data

always generate the same output for a given input (deterministic). There are a variety of human-designed features in the cheminformatics literature, many of which are close variations of the two that we consider: **ECFP** [28] and **Mordred** [24]. We do not consider the "PubChem" fingerprint [3], as it was shown to have less feature importance for tree models compared to other cheminformatics descriptors [32]. Learned feature descriptors, such as **Mol2vec** [17], were first inspired by Natural Language Processing (NLP), with newer ones using transformers, like **ChemBERTa-2** [5, 4] and **MTL-BERT** [41]. Finally, self-supervised learning on graphs [35] has been used to create **InfoMax2D** [14] and **InfoGraph3D** [30] features, which we also test. Each of these feature extractors can be used together with a variety of classical machine learning methods, such as **SVMs** [6], decision trees (**Random Forests (RF)** and **Light Gradient Boosting Machine (LGBM)** [19]), **K-Nearest Neighbours (KNN)**, **Gaussian Processes (GP)** [27], and **Multilayer Perceptrons (MLP)**.

Deep learning methods Deep learning methods such as GNNs have surged in popularity in drug discovery due to their ability to directly work on the 2D graph representation of molecular structure. In theory, this should allow the most effective features to be learned from data. Here, we included a number of architectures: **Directed Message Passing Neural Networks (D-MPNN)** [39], **Graph Convolutional Networks (GCN)** [21], **Attentive Fingerprint (A-FP)** [38], and **Graph Attention Networks (GAT)** [34]. Other deep learning methods such as LSTMs and CNNs have previously been assessed in this domain [33]; we chose not to include them in our benchmark as these model architectures have been superseded by transformer-based models in recent years.

3.2 Conclusions and Recommendations from Past Literature

Multiple publications have compared machine learning methods for molecular property predictions. Here, we outline the most important works and their findings.

Graph Neural Networks are currently widely studied in the hope that feature learning directly on the molecular graph leads to better performance. Recent works [43, 36, 39] show continuous improvement in GNN performance on MoleculeNet regression datasets [36]. GNNs are often only compared to other GNNs [30], or on a single benchmark dataset [22], preventing general conclusions in a wider context. Yang et al. [39] compare GNNs to classical methods (RFs and MLPs – a subset of those in section 3.1) on MoleculeNet, and find that in 1 out of 3 regression datasets GNNs perform best. Jiang et al. [18] on the other hand, report the same GNN method being outperformed by SVMs. In [36], where MoleculeNet was originally introduced, it was found that XGBoost performed the best. It is difficult to draw conclusions across papers where different subsets of models are compared each time. More recently, pre-trained deep learning models [17, 41, 5, 4] showed promise, with e.g. Ahmad et al. [4] demonstrating improvements in performance over classical models in 3 of 4 datasets.

Papers centred on a particular application, such as TDC, often perform more comprehensive benchmarks using classical methods. Huang et al. [15] introduce the TDC datasets and benchmark molecular descriptors and graph based models, with different methods working best in different situations. Later, Tian et al. [32] showed XGBoost models were highly performant across a range of the TDC benchmarks. Similarly, van Tilborg et al. [33] introduced the MoleculeACE datasets, and showed classical models (SVMs) combined with ECFP outperforming all deep learning models. Griffiths et al. [12] suggest that Gaussian processes can also be performant, but only compare to simple (Bayesian) neural networks.

Finally, only a small subset of studies evaluate methods that explicitly quantify uncertainty [8, 43, 12]. For practitioners, uncertainty around model predictions is a key metric when prioritising molecules for synthesis and experimentation. There are numerous ways to encapsulate uncertainty in models. For instance, variability among ensemble members [8], leveraging inherent variance in GPs, [12], and Dropout Variational Inference or Stein Variational Gradient Descent for GNNs [43]. However, the metrics used for uncertainty quantification tend to diverge significantly between studies so that no clear picture has emerged, yet.

4 Experimental Procedures

4.1 Set-up and configuration

In our study, we developed a Python-based pipeline for comprehensively comparing various methods and models for drug property regression tasks, addressing the inconsistencies and gaps in the current

literature (see section 3.1). We aimed to use each model as it would be used in a real setting, giving each model the highest chances of scoring top on a given dataset (those discussed in section 2). Therefore, each model is provided with training data alone, and the handling of the data is optimised for the model in question. For instance, GPs in real-world applications do not require validation data and can therefore use all the training data to build a model, while a GNN training loop requires validation data to prevent overfitting, thereby sacrificing some training data. In the context of real-world applications, we consider this procedure to be the fairest way to compare models.

As discussed in section 3.2, only a small number of papers investigate uncertainty quantification. The simplest way to extract an uncertainty measurement for a given prediction is to train an ensemble of models and measure the variance in the models’ predictions. Therefore, in addition to training single models, we also trained a corresponding ensemble of models for each model type. This enabled us to estimate uncertainty while potentially improving the associated point prediction. Despite ensembles improving uncertainty estimation, their predictive variance may be *uncalibrated*, and not match the variance of the future testing data [25]. We also consider further improving the uncertainty estimates of ensembles through a post-hoc calibration procedure, at the cost of requiring an additional holdout calibration dataset. Similar to models that require validation data at training time, calibrated models sacrifice training data. This reduces the amount of training data available for optimising model parameters, possibly presenting a trade-off between inhibited model performance and improved uncertainty estimates.

This resulted in any base model (SVM, GP, GNN, etc.) having 4 distinct model flavours: Single Model, Ensemble Model, Calibrated Single Model and Calibrated Ensemble Model. Our model library included SVM, RF, KNN (sklearn, 1.0.2), LGBM ([19] 3.3.5), GP (GPyTorch [9], 1.8.1), MLP, A-FP, GAT, GCN, and D-MPNN (DeepChem [26], 2.7.1). Each model was paired with featurisers such as graphs [26] (MGC and D-MPNN for GNNs only), Extended-Connectivity Fingerprints (ECFP, radius 2, number of bits 1024), Mordred [24], and Mol2Vec [17]. We also used pre-trained graph models and transformers as featurisers. InfoMax2D was trained in-house based on previous literature [35, 14]. InfoGraph3D was pre-trained on the Drugs database as outlined in [30]. ChemBERTa-2 was used directly from Hugging Face [5] (ChemBERTa-77M-MTR). MTL-BERT was trained on 2 million compounds from ChEMBL [10] as in [42].

Ensemble models were trained with 3 base models. We conducted a random search with 3-fold cross-validation over a hyperparameter search space of 20 hyperparameter combinations to optimise model performance. Deep learning models were trained for 300 epochs with an early stopping schedule of no new lowest validation loss for 50 consecutive epochs. Models requiring validation and/or calibration sets used an 80/20 random split. For each dataset, models were trained using all compatible model-featuriser sets. In total 184 descriptor and model combinations were trained for each dataset. A cluster of 40 NVIDIA T4 GPUs was used for parallelised training across datasets, with models for each dataset being trained on a single GPU.

4.2 Uncertainty Quantification, Evaluation, and Calibration

We are interested in quantifying uncertainty because this helps decision makers balance risk. For example, when searching for a compound with desired properties, experiments in unexplored regions (with high uncertainty) should be balanced with experiments in known promising regions. This procedure, even when performed with human input, is somewhat like Bayesian optimisation [13], and uncertainty is crucial for balancing exploration and exploitation. If a method’s predictive distribution matches the frequency of outcomes in the future, optimal decisions can be made.

For evaluation, we use *proper scoring rules* [11], which have the property that they are minimised only when the predictive distribution matches the test set distribution. This allows the quality of a probabilistic forecast to be summarised in a single number that combines accuracy and the quality of uncertainty estimate. This is unlike pure calibration metrics (e.g. expected calibration error, or ECE, for classification), which can be maximised even if predictions have the accuracy of a random guess. We choose the “negative log predictive density” (NLPD) scoring rule, which has a clear interpretation as the return from a repeated betting game where resources need to be spread across different bets [20]. We chose this as a proxy for spreading resources among developing different compounds.

Our predictive distributions quantify both epistemic (model uncertainty) and aleatoric (inherent system or process uncertainty) uncertainty [7]. An estimate of aleatoric uncertainty can be found for

all methods by calculating the mean-squared error on the training data, and using this as the variance in a noise model, i.e. given the prediction $f(x^*)$ we model our observation y^* as

$$p(y^*|f(x^*)) = \mathcal{N}(y; f(x^*), \sigma^2), \quad \sigma^2 = \frac{1}{N} \sum_{n=1}^N (f(x_n^{\text{train}}) - y_n^{\text{train}})^2. \quad (1)$$

For ensemble models, we estimate the epistemic uncertainty in the prediction again as a Gaussian distribution, with mean and variance given by that across the ensemble components:

$$p(f(x^*)|\text{data}) \approx \mathcal{N}(f(x^*); \mu(x^*), \nu(x^*)), \quad (2)$$

$$\mu(x^*) = \frac{1}{K} \sum_{k=1}^K f_k^{\text{ens}}(x^*), \quad \nu(x^*) = \frac{1}{K} \sum_{k=1}^K (f_k^{\text{ens}}(x^*) - \mu(x^*))^2. \quad (3)$$

Gaussian processes provide a direct calculation of $p(f(x^*)|\text{data})$ [27]. Using this predictive distribution, we can calculate the NLPD score as

$$\text{NLPD} = -\frac{1}{N_{\text{test}}} \sum_{n=1}^{N_{\text{test}}} \log \mathcal{N}(y_n^{\text{test}}; \mu(x_n^{\text{test}}), \nu(x_n^{\text{test}}) + \sigma^2). \quad (4)$$

In cases where predictions are systematically over/underconfident, also consider calibrating the models on a hold-out calibration set. To do this, we scale the predicted mean and variance to make the scaled residuals $(y_n^{\text{test}} - \mu(x_n^{\text{cal}}))/\sqrt{\nu(x_n^{\text{cal}}) + \sigma^2}$ have zero empirical mean and unit empirical variance. When considering only rescaling, this minimises NLPD on the calibration set.

5 Experimental Results and Discussion

5.1 Which machine learning model, across the broad spectrum of existing models, consistently exhibits superior performance in a variety of datasets?

We trained all of our uncalibrated descriptor-model combinations on each of our QSAR and ADME(T) datasets (section 3). We compared model performance using the root mean squared error normalised by the interquartile range of the training data ($\text{NRMSE} = \frac{\text{RMSE}_{\text{test}}}{\text{IQR}_{\text{train}}}$). The NRMSE enables direct comparison of performance across datasets and can be interpreted as the "predictive resolution" of a model, i.e., the resolution to which accurate predictions can be made. The IQR was chosen as the normalisation constant due to its robustness to outliers compared to the standard deviation. The training data can be viewed as a representative sample from the true underlying population in both feature and target space. For ($\text{NRMSE} < 1$) the mean error is less than the spread of the prediction target. Conversely, an ($\text{NRMSE} > 1$) indicates that the expected error in the prediction is greater than the IQR of the training data indicating poor performance. A numerical summary of experimental results is given in Table A.2.

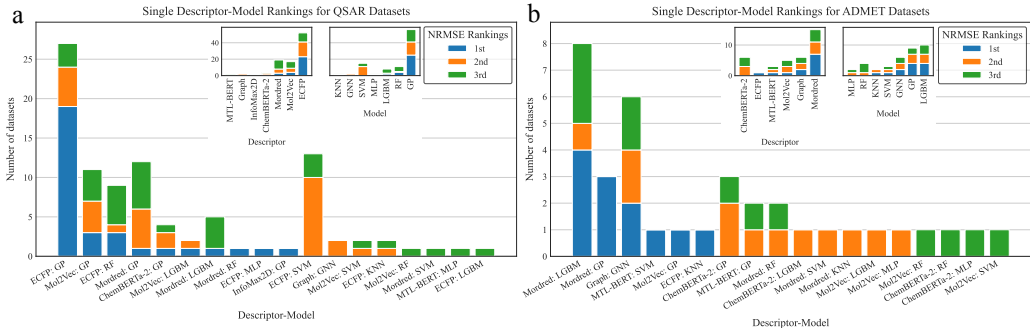


Figure 1: Single descriptor-model rankings based on NRMSE for a) QSAR datasets and b) ADME(T) datasets. Each count corresponds to the number of datasets on which a descriptor-model combination ranked as 1st, 2nd, or 3rd by NRMSE. The inset illustrates the same but for each descriptor and model independently. Higher numbers indicate better performance.

The 3 top performing models by NRMSE were identified for each dataset; these rankings are shown in Figure 1, ordered according to the number of datasets in which they secured the 1st position, followed by the 2nd, and 3rd. Ensemble models are excluded from these results as we observed no statistically significant difference in NRMSE between ensemble and single models (two-sided paired t-tested: $\alpha = 0.05, p = 0.419$, Figure 3b), in agreement with previous literature [8].

For QSAR datasets, we found that GPs with ECFP descriptors achieved first place in the majority of datasets (1st in 19/32 and 2nd or 3rd in 8/32, Figure 1a). Irrespective of descriptor, GPs were ranked top in 25/32 datasets (Figure 1a inset). The superior performance of GPs for QSAR data in particular is a key finding as many studies that compare classical methods with deep learning techniques neglect to include GPs [33, 18, 5]. Our analysis also identified SVMs and ECFP as the most frequent 2nd ranked descriptor-model combination, consistent with van Tilborg et al. [33] (Figure 1a).

For ADME(T) datasets, there was more variability in top performing descriptors and models. Mordred descriptors emerged as the most effective feature space for these datasets, especially when used with LGBMs (Figure 1b). GNNs and GPs also performed well across these datasets (Figure 1b). In contrast to QSAR datasets, SVMs and ECFP descriptors appear unable to effectively capture molecular information for these datasets. Additionally, we discovered that NLP-based descriptors (Mol2Vec, MTL-BERT, ChemBERTa-2) performed well on these datasets even when compared to ECFP, in agreement with literature [33, 41, 5, 18]. Our results suggest that the most effective molecular representation is ECFP for QSAR datasets and dataset dependent for ADME(T).

5.2 Do specific models demonstrate enhanced performance on particular types of datasets?

Figure 1 provides a measure of model performance, however, this does not describe the magnitude of performance increase in selecting the 1st ranked model, compared to the 2nd or 3rd or indeed models outside of the top 3. Figure 2 shows quantitative measurements of model performance, where for each dataset the NRMSE for each trained model is shown with the top 3 models highlighted.

For QSAR datasets, there is a notable performance gap between the top performing models and all others, with only small differences between the best models (Figure 2a). For ADME(T) datasets (Figure 2b), the best performing model varies by dataset, indicated by a variety of colours amongst the top performing models. NRMSE values are generally greater than for QSAR datasets, suggesting it is more difficult to predict accurately on ADME(T) datasets (Figure 2b). As with QSAR datasets, there is generally a notable gap in performance between the best performing models and all others. Where there is a noteworthy difference in performance between the top models, GNNs are often the best performers, e.g. in the *lipo* (in agreement with [18]) and *ld50_zhu* datasets, indicating that they are in fact well suited to a specific subset of datasets. The *ppbr_az** dataset appears to be particularly challenging to predict with an NRMSE > 1 (NRMSE = 1.07). However, this is still an improvement over a naïve prediction of the training data mean for all test points, which gives $\text{NRMSE}_{\text{mean}} = 1.30$.

5.3 Which models best quantify uncertainty in their predictions?

As discussed in section 4, we aim to develop models with good uncertainty estimates, as well as good mean predictions. So in addition to measuring NRMSE, we also measure NLPD, which measures *both* accuracy and uncertainty quantification. Considering this additional metric may complicate drawing conclusions about “best” models, as the model with the best mean predictions may have poor uncertainty estimates. To assess whether this is the case, the comparison based on NRMSE in Figure 2 has the model with the best NLPD highlighted by a star. For the QSAR datasets, we see that the model with the best uncertainty quantification always has the best, or one of the best NRMSEs. For some ADME(T) datasets (in particular *freesolv*, *ld50_zhu* and *clearance_hepatocyte_az*), the best models by NLPD are outside the top 3. These demonstrate instances where the NRMSE decreases when selecting the best model by NLPD. Therefore, for certain ADME(T) datasets, it might be necessary to strike a balance between the point prediction accuracy and the estimation of uncertainty.

Next, we directly compare the NLPD of all models, including ensemble versions of all methods that do not naturally provide uncertainty estimates (i.e. all methods except GPs). Ensembles are known to improve uncertainty estimates without reducing predictive accuracy (verified in Figure 3a). Ensembled GPs do not improve uncertainty quantification (verified in Figure 3b), leading them to be excluded from the comparisons. Since the raw uncertainty values from ensembles are known to contain bias (as shown by Palmer et al. [25]), we also consider calibrated versions of these models, in

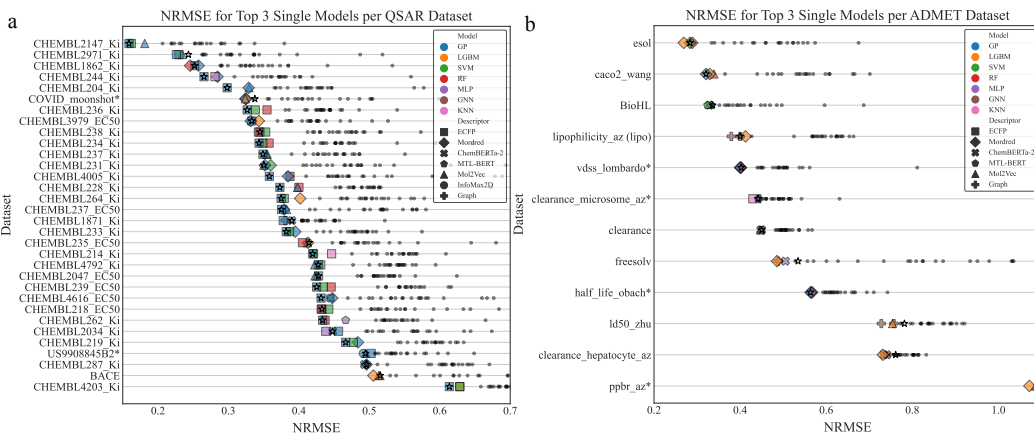


Figure 2: NRMSE for the top 3 single models for each dataset, split into a) QSAR datasets, and b) ADME(T) datasets. Colour and shape indicate model and descriptor type respectively. Lower NRMSE values (towards the left) indicate better performance. An asterisk (*) indicates that the target values have been log-transformed. The smaller black points correspond to models that did not appear in the top 3, but still fall within the axes limits. Stars (★) indicate the NRMSE score for model with the best uncertainty quantification, as measured by NLPD.

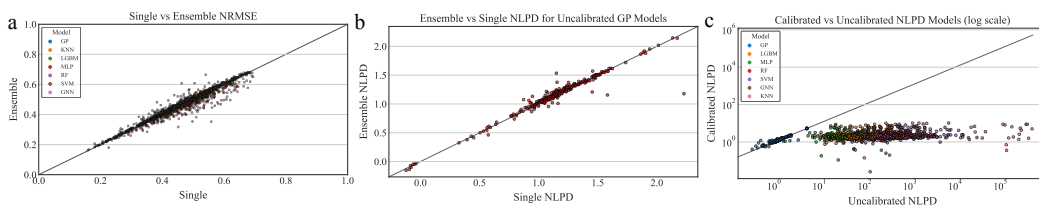


Figure 3: a) NRMSE for corresponding single and ensemble models b) NLPD for corresponding single and ensemble GPs. For both a) and b), points below the line indicate that ensembling improved performance compared to a single model c) NLPD for corresponding calibrated and uncalibrated models (single for GPs, ensemble for all others). Points below the line indicate that calibration improved performance compared to leaving a model uncalibrated. Data is shown for all datasets.

order to maximally benefit from the signal in ensembles’ uncertainty. Figure 3c shows that calibration greatly improves NLPD for ensemble models, while making little difference for GP models.

Based on these observations, we compare the NLPD in Figure 4 for all ensembled+calibrated models, and calibrated and uncalibrated GPs. For QSAR datasets, both calibrated and uncalibrated GPs provide the most accurate uncertainty estimates, by a wide margin when compared to the best non-GP models (Figure 4a). Selecting a model based on the best NRMSE (highlighted by a star) almost always results in good uncertainty estimation (low NLPD). This is consistent with Figure 2, and is unsurprising given that GPs tend to be the best performers for QSAR datasets in both point and uncertainty prediction (Figure 2a and Figure 4a, respectively). For ADME(T) datasets, the results are broadly similar, however there are cases where GPs are outperformed by GNNs and MLPs (*ppbr_az** and *freesolv* datasets Figure 4b). Selecting a model based on the best NRMSE does not always result in good uncertainty estimation for these datasets, meaning a compromise may be necessary to balance the quality of point and uncertainty estimates for these property classes.

5.4 What are the trade-offs between computational time and performance?

Drug property prediction datasets are usually small, with the datasets used in this work consisting of between approximately 50 and 3500 data points. Limitations on training and inference time depend on the practitioner’s personal requirements. Nevertheless, we provide an overview of featurisation, training and inference time for the descriptors and models used here as a general guide as calculated on our hardware (optimised using GPU acceleration for both training and inference for GNNs, GPs and

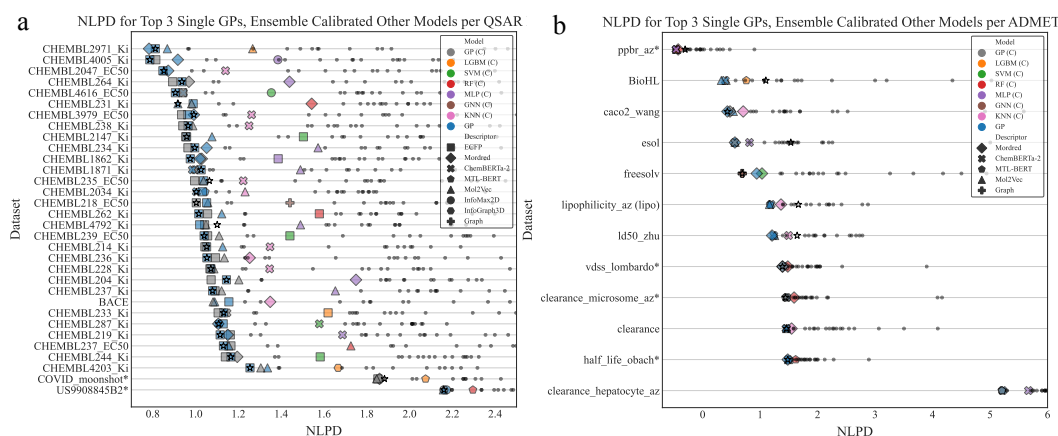


Figure 4: NLPD for the top 3 single models for each dataset, split into a) QSAR datasets, and b) ADME(T) datasets. Colour indicates model type, and shape descriptor type. Lower NLPD values (towards the left) indicate better performance. An asterisk (*) indicates that the target values have been log-transformed. The smaller black points correspond to models that did not appear in the top 3, but still fall within the axes limits. Stars (☆) indicate the NLPD for the most accurate model based on NRMSE. The top performing non-GP model by NLPD for each dataset is also highlighted if all 3 best performing models are GPs. Calibrated models are indicated by (C).

MLPs, CPU parallelisation for LGBMs and RFs and single threaded CPU otherwise). Computation of the following descriptors in seconds took: 10^0 (ECFP), 10^1 (ChemBERTa-2, MTL-BERT, Mol2Vec, InfoMax2D, InfoGraph3D, Graph), 10^3 (Mordred). Training of the following single models in seconds took: 10^0 (KNN, MLP), 10^1 (GP, LGBM, SVM), 10^3 (RF, GNN). Inference using the following single models in seconds took: 10^{-2} (GP, MLP), 10^{-1} (LGBM, RF, KNN), 10^0 (RF, GNN), 10^1 (SVM). Detailed summaries of runtimes are given in Figure A.1.

6 Conclusions and Future Directions

Our comprehensive evaluation of machine learning methods on a broad selection of benchmark datasets aimed to address the inconsistencies and gaps in the literature for drug property regression tasks. Our results demonstrated that the effectiveness of a particular model is dependent on the property class and the feature descriptors used.

The most striking finding was the superior performance of GPs on QSAR datasets, particularly in conjunction with ECFP descriptors. Despite being often overlooked in benchmarking studies, GPs not only excelled in point prediction but also provided the most accurate uncertainty estimates. This underlines the importance of considering GPs as viable models for QSAR datasets. However, for ADME(T) datasets, the choice of the optimal model was less clear. The results suggested that GNNs can lead to very good results and that LGBMs and GPs perform well with Mordred descriptors. For ADME(T) datasets, there was a notable trade-off between point prediction accuracy and uncertainty estimation as improving uncertainty decreased accuracy and vice versa.

Some notable limitations of our study were that we did not investigate more complex ensemble methods, different calibration techniques, or pre-training followed by fine-tuning. Moreover, we did not explore other methods for uncertainty estimation, such as hyperplane distance for SVMs or variance in Random Forests. For deep learning models, techniques such as dropout, weight priors, or Stein Variational Gradient Descent could also be investigated.

In conclusion, our study highlights the importance of carefully selecting models based on the specific property at hand and the necessity of uncertainty quantification in drug property prediction tasks. Ideally, this approach requires an automatic framework for model training, testing and selection in order to deliver the best performance for a specific dataset and property class. Future work should aim to expand on these findings, exploring new models, calibration methods, and uncertainty estimation techniques. This would help to further accelerate, de-risk and facilitate more effective decision-making in the drug discovery process.

References

- [1] URL <https://pubchem.ncbi.nlm.nih.gov/patent/US-9908845-B2>.
- [2] Mar 2023. URL <https://dndi.org/research-development/portfolio/covid-moonshot/>.
- [3] Pubchem substructure fingerprint. ftp://ftp.ncbi.nlm.nih.gov/pubchem/specifications/pubchem_fingerprints.pdf, 2023. Accessed: May. 2023.
- [4] Walid Ahmad, Elana Simon, Seyone Chithrananda, Gabriel Grand, and Bharath Ramsundar. Chemberta-2: Towards chemical foundation models, 2022.
- [5] Seyone Chithrananda, Gabriel Grand, and Bharath Ramsundar. Chemberta: Large-scale self-supervised pretraining for molecular property prediction, 2020.
- [6] Corinna Cortes and Vladimir Vapnik. Support-vector networks. *Machine learning*, 20(3): 273–297, 1995.
- [7] Armen Der Kiureghian and Ove Ditlevsen. Aleatory or epistemic? does it matter? *Structural safety*, 31(2):105–112, 2009.
- [8] Thomas-Martin Dutschmann, Lennart Kinzel, Antonius Ter Laak, and Knut Baumann. Large-scale evaluation of k-fold cross-validation ensembles for uncertainty estimation. *Journal of Cheminformatics*, 15(1):49, 2023.
- [9] Jacob R Gardner, Geoff Pleiss, David Bindel, Kilian Q Weinberger, and Andrew Gordon Wilson. Gpytorch: Blackbox matrix-matrix gaussian process inference with gpu acceleration. In *Advances in Neural Information Processing Systems*, 2018.
- [10] Anna Gaulton, Anne Hersey, Michał Nowotka, A Patrícia Bento, Jon Chambers, David Mendez, Prudence Mutowo, Francis Atkinson, Louisa J Bellis, Elena Cibrián-Uhalte, et al. The chembl database in 2017. *Nucleic acids research*, 45(D1):D945–D954, 2017.
- [11] Tilmann Gneiting and Adrian E Raftery. Strictly proper scoring rules, prediction, and estimation. *Journal of the American statistical Association*, 102(477):359–378, 2007.
- [12] Ryan-Rhys Griffiths, Leo Klärner, Henry B. Moss, Aditya Ravuri, Sang Truong, Samuel Stanton, Gary Tom, Bojana Rankovic, Yuanqi Du, Arian Jamasb, Aryan Deshwal, Julius Schwartz, Austin Tripp, Gregory Kell, Simon Frieder, Anthony Bourached, Alex Chan, Jacob Moss, Chengzhi Guo, Johannes Durholt, Saudamini Chaurasia, Felix Strieth-Kalthoff, Alpha A. Lee, Bingqing Cheng, Alán Aspuru-Guzik, Philippe Schwaller, and Jian Tang. Gauche: A library for gaussian processes in chemistry. 2022.
- [13] Philipp Hennig, Michael A Osborne, and Hans P Kersting. *Probabilistic Numerics: Computation as Machine Learning*. Cambridge University Press, 2022.
- [14] Weihua Hu, Bowen Liu, Joseph Gomes, Marinka Zitnik, Percy Liang, Vijay Pande, and Jure Leskovec. Strategies for pre-training graph neural networks. 2020.
- [15] Kexin Huang, Tianfan Fu, Wenhao Gao, Yue Zhao, Yusuf Roohani, Jure Leskovec, Connor W Coley, Cao Xiao, Jimeng Sun, and Marinka Zitnik. Therapeutics data commons: Machine learning datasets and tasks for drug discovery and development. *Proceedings of Neural Information Processing Systems, NeurIPS Datasets and Benchmarks*, 2021.
- [16] Kexin Huang, Tianfan Fu, Wenhao Gao, Yue Zhao, Yusuf Roohani, Jure Leskovec, Connor W Coley, Cao Xiao, Jimeng Sun, and Marinka Zitnik. Artificial intelligence foundation for therapeutic science. *Nature Chemical Biology*, 2022.
- [17] Sabrina Jaeger, Simone Fulle, and Samo Turk. Mol2vec: unsupervised machine learning approach with chemical intuition. *Journal of chemical information and modeling*, 58(1):27–35, 2018.
- [18] Dejun Jiang, Zhenxing Wu, Chang-Yu Hsieh, Guangyong Chen, Ben Liao, Zhe Wang, Chao Shen, Dongsheng Cao, Jian Wu, and Tingjun Hou. Could graph neural networks learn better molecular representation for drug discovery? a comparison study of descriptor-based and graph-based models. *Journal of cheminformatics*, 13(1):1–23, 2021.
- [19] Guolin Ke, Qi Meng, Thomas Finley, Taifeng Wang, Wei Chen, Weidong Ma, Qiwei Ye, and Tie-Yan Liu. Lightgbm: A highly efficient gradient boosting decision tree. In I. Guyon,

- U. Von Luxburg, S. Bengio, H. Wallach, R. Fergus, S. Vishwanathan, and R. Garnett, editors, *Advances in Neural Information Processing Systems*, volume 30. Curran Associates, Inc., 2017. URL https://proceedings.neurips.cc/paper_files/paper/2017/file/6449f44a102fde848669bdd9eb6b76fa-Paper.pdf.
- [20] John L Kelly. A new interpretation of information rate. *the bell system technical journal*, 35(4): 917–926, 1956.
- [21] Thomas N Kipf and Max Welling. Semi-supervised classification with graph convolutional networks. *arXiv preprint arXiv:1609.02907*, 2016.
- [22] Junying Li, Deng Cai, and Xiaofei He. Learning graph-level representation for drug discovery. *arXiv preprint arXiv:1709.03741*, 2017.
- [23] Kamel Mansouri, Chris M Grulke, Richard S Judson, and Antony J Williams. Opera models for predicting physicochemical properties and environmental fate endpoints. *Journal of cheminformatics*, 10(1):1–19, 2018.
- [24] Hiroto Moriwaki, Yu-Shi Tian, Norihito Kawashita, and Tatsuya Takagi. Mordred: a molecular descriptor calculator. *Journal of cheminformatics*, 10(1):1–14, 2018.
- [25] Glenn Palmer, Siqi Du, Alexander Politowicz, Joshua Paul Emory, Xiyu Yang, Anupraas Gautam, Grishma Gupta, Zhelong Li, Ryan Jacobs, and Dane Morgan. Calibration after bootstrap for accurate uncertainty quantification in regression models. *npj Computational Materials*, 8(1):115, 2022.
- [26] Bharath Ramsundar, Peter Eastman, Patrick Walters, Vijay Pande, Karl Leswing, and Zhenqin Wu. *Deep Learning for the Life Sciences*. O’Reilly Media, 2019. <https://www.amazon.com/Deep-Learning-Life-Sciences-Microscopy/dp/1492039837>.
- [27] Carl Edward Rasmussen and Christopher KI Williams. *Gaussian processes for machine learning*, volume 2. MIT press Cambridge, MA, 2006.
- [28] David Rogers and Mathew Hahn. Extended-connectivity fingerprints. *Journal of chemical information and modeling*, 50(5):742–754, 2010.
- [29] Robert P. Sheridan, Wei Min Wang, Andy Liaw, Junshui Ma, and Eric M. Gifford. Extreme gradient boosting as a method for quantitative structure–activity relationships. *Journal of Chemical Information and Modeling*, 56(12):2353–2360, 2016. doi: 10.1021/acs.jcim.6b00591.
- [30] Hannes Stärk, Dominique Beaini, Gabriele Corso, Prudencio Tossou, Christian Dallago, Stephan Günnemann, and Pietro Liò. 3d infomax improves gnns for molecular property prediction. 2022.
- [31] Ruoxi Sun, Hanjun Dai, and Adams Wei Yu. Does gnn pretraining help molecular representation? 2022.
- [32] Hao Tian, Rajas Ketkar, and Peng Tao. Accurate admet prediction with xgboost. 2022.
- [33] Derek van Tilborg, Alisa Alenicheva, and Francesca Grisoni. Exposing the limitations of molecular machine learning with activity cliffs. *Journal of Chemical Information and Modeling*, 62(23):5938–5951, 2022.
- [34] Petar Veličković, Guillem Cucurull, Arantxa Casanova, Adriana Romero, Pietro Lio, and Yoshua Bengio. Graph attention networks. *arXiv preprint arXiv:1710.10903*, 2017.
- [35] Petar Veličković, William Fedus, William L. Hamilton, Pietro Liò, Yoshua Bengio, and R Devon Hjelm. Deep graph infomax. 2018.
- [36] Zhenqin Wu, Bharath Ramsundar, Evan N. Feinberg, Joseph Gomes, Caleb Geniesse, Aneesh S. Pappu, Karl Leswing, and Vijay Pande. Moleculenet: a benchmark for molecular machine learning. *Chem. Sci.*, 9:513–530, 2018.
- [37] Zhenxing Wu, Tailong Lei, Chao Shen, Zhe Wang, Dongsheng Cao, and Tingjun Hou. Admet evaluation in drug discovery. 19. reliable prediction of human cytochrome p450 inhibition using artificial intelligence approaches. *Journal of Chemical Information and Modeling*, 59(11): 4587–4601, 2019. doi: 10.1021/acs.jcim.9b00801.
- [38] Zhaoping Xiong, Dingyan Wang, Xiaohong Liu, Feisheng Zhong, Xiaozhe Wan, Xutong Li, Zhaojun Li, Xiaomin Luo, Kaixian Chen, Hualiang Jiang, et al. Pushing the boundaries of molecular representation for drug discovery with the graph attention mechanism. *Journal of medicinal chemistry*, 63(16):8749–8760, 2019.

- [39] Kevin Yang, Kyle Swanson, Wengong Jin, Connor Coley, Philipp Eiden, Hua Gao, Angel Guzman-Perez, Timothy Hopper, Brian Kelley, Miriam Mathea, et al. Analyzing learned molecular representations for property prediction. *Journal of chemical information and modeling*, 59(8):3370–3388, 2019.
- [40] Jin Zhang, Daniel Mucs, Ulf Norinder, and Fredrik Svensson. Lightgbm: An effective and scalable algorithm for prediction of chemical toxicity—application to the tox21 and mutagenicity data sets. *Journal of Chemical Information and Modeling*, 59(10):4150–4158, 2019. doi: 10.1021/acs.jcim.9b00633.
- [41] Xiao-Chen Zhang, Cheng-Kun Wu, Jia-Cai Yi, Xiang-Xiang Zeng, Can-Qun Yang, Ai-Ping Lu, Ting-Jun Hou, and Dong-Sheng Cao. Pushing the boundaries of molecular property prediction for drug discovery with multitask learning bert enhanced by smiles enumeration. *Research*, 2022:0004, 2022.
- [42] Xuan Zhang. Mtl-bert: Multi-task learning with bert, 2023. URL <https://github.com/zhang-xuan1314/MTL-BERT>. GitHub repository.
- [43] Yao Zhang and Alpha A. Lee. Bayesian semi-supervised learning for uncertainty-calibrated prediction of molecular properties and active learning. *Chem. Sci.*, 10:8154–8163, 2019. doi: 10.1039/C9SC00616H. URL <http://dx.doi.org/10.1039/C9SC00616H>.

A Appendix

A.1 Datasets Summary

Table A.1: Dataset Summary (44 total). Datasets where the target values have been log-transformed are suffixed with an asterisk (*).

Dataset	Property	Train/Test Split	Dataset Size	Train Size	Test Size	Source	Reference
BACE	Affinity	DeepChem	1513	1361	152	DeepChem	[26]
BioHL	ADME(T)(Metabolism)	Opera	150	112	38	OPERA	[23]
caco2_wang	ADME(T)(Absorption)	TDC (Scaffold)	906	725	181	TDC	[15]
CHEMBL1862_Ki	Affinity	ACE	794	633	161	MoleculeACE	[33]
CHEMBL1871_Ki	Affinity	ACE	659	525	134	MoleculeACE	[33]
CHEMBL2034_Ki	Affinity	ACE	750	598	152	MoleculeACE	[33]
CHEMBL204_Ki	Affinity	ACE	2754	2201	553	MoleculeACE	[33]
CHEMBL2047_EC50	Affinity	ACE	631	503	128	MoleculeACE	[33]
CHEMBL214_Ki	Affinity	ACE	3321	2655	666	MoleculeACE	[33]
CHEMBL2147_Ki	Affinity	ACE	1456	1162	294	MoleculeACE	[33]
CHEMBL218_EC50	Affinity	ACE	1031	823	208	MoleculeACE	[33]
CHEMBL219_Ki	Affinity	ACE	1867	1492	375	MoleculeACE	[33]
CHEMBL228_Ki	Affinity	ACE	1704	1362	342	MoleculeACE	[33]
CHEMBL231_Ki	Affinity	ACE	973	776	197	MoleculeACE	[33]
CHEMBL233_Ki	Affinity	ACE	3142	2512	630	MoleculeACE	[33]
CHEMBL234_Ki	Affinity	ACE	3659	2925	734	MoleculeACE	[33]
CHEMBL235_EC50	Affinity	ACE	2353	1880	473	MoleculeACE	[33]
CHEMBL236_Ki	Affinity	ACE	2598	2077	521	MoleculeACE	[33]
CHEMBL237_EC50	Affinity	ACE	955	762	193	MoleculeACE	[33]
CHEMBL237_Ki	Affinity	ACE	2603	2081	522	MoleculeACE	[33]
CHEMBL238_Ki	Affinity	ACE	1052	839	213	MoleculeACE	[33]
CHEMBL239_EC50	Affinity	ACE	1727	1380	347	MoleculeACE	[33]
CHEMBL244_Ki	Affinity	ACE	3097	2476	621	MoleculeACE	[33]
CHEMBL262_Ki	Affinity	ACE	856	683	173	MoleculeACE	[33]
CHEMBL264_Ki	Affinity	ACE	2862	2288	574	MoleculeACE	[33]
CHEMBL287_Ki	Affinity	ACE	1328	1061	267	MoleculeACE	[33]
CHEMBL2971_Ki	Affinity	ACE	976	779	197	MoleculeACE	[33]
CHEMBL3979_EC50	Affinity	ACE	1133	905	228	MoleculeACE	[33]
CHEMBL4005_Ki	Affinity	ACE	960	767	193	MoleculeACE	[33]
CHEMBL4203_Ki	Affinity	ACE	731	582	149	MoleculeACE	[33]
CHEMBL4616_EC50	Affinity	ACE	682	543	139	MoleculeACE	[33]
CHEMBL4792_Ki	Affinity	ACE	1471	1174	297	MoleculeACE	[33]
clearance_hepatocyte_az_tpad	ADME(T)(Excretion)	TDC (Scaffold)	1020	817	203	TDC	[15]
clearance_microsome_az_tpad*	ADME(T)(Excretion)	TDC (Scaffold)	1102	881	221	TDC	[15]
clearance	ADME(T)(Excretion)	DeepChem	837	753	84	DeepChem	[26]
COVID_moonshot*	Affinity	MinMax	2063	1573	353	Covid Moonshot	[2]
esol	ADME(T)(Absorption)	DeepChem	1117	1004	113	DeepChem	[26]
freesolv	ADME(T)(Absorption)	DeepChem	642	577	65	DeepChem	[26]
half_life_obach*	ADME(T)(Excretion)	TDC (Scaffold)	665	531	134	TDC	[15]
ld50_zhu	ADME(T)(Toxicity)	TDC (Scaffold)	7342	5876	1466	TDC	[15]
lipophilicity_astazeneca	ADME(T)(Absorption)	TDC (Scaffold)	4200	3360	840	TDC	[15]
ppbr_az*	ADME(T)(Distribution)	TDC (Scaffold)	1797	1454	343	TDC	[15]
US9908845B2*	Affinity	MinMax	335	251	84	Patent Data	[1]
vdss_lombardo*	ADME(T)(Distribution)	TDC (Scaffold)	1111	890	221	TDC	[15]

A.2 Numerical Results for Best Performing Models

Table A.2: Full results of top 3 performing models by dataset if ranked by best (lowest) NRMSE or by best (lowest) NLPD. Datasets where the target values have been log-transformed are suffixed with an asterisk (*). Calibrated models are indicated by (C). All results are given to 4 significant figures, except hyperparameter optimisation and training time, which are given to 2 significant figures.

Dataset	Property Class	Best By	Rank	Descriptor	Model	MSE	RMSE	NRMSE	Pearson R	NLPD	Featurisation (s)	Hyperparameter Optimisation (s)	Training (s)	Inference (s)
BioHL	ADME(T)	NRMSE	1st	MTL-BERT	SVM	0.1118	0.3343	0.3244	0.9034	18.71	13	0.35	0.009481	0.006161
			2nd	ChemBERTa-2	GP	0.1147	0.3386	0.3286	0.8977	0.3944	1.4	68	1.586	0.00407
			3rd	MTL-BERT	GP	0.1177	0.3431	0.3329	0.9001	0.4507	13	74	0.5088	0.004628
	NLPD	1st	Mol2Vec	GP	0.12	0.3465	0.3362	0.8967	0.3263	2.5	61	0.4085	0.003968	0.4085
		2nd	ChemBERTa-2	GP	0.1147	0.3386	0.3286	0.8977	0.3944	1.4	68	1.586	0.00407	1.586
		3rd	Mol2Vec	GP (C)	0.1263	0.3554	0.3449	0.8852	0.408	2.5	61	1.503	0.007095	1.503
caco2_wang	ADME(T)	NRMSE	1st	Mordred	GP	0.1254	0.3542	0.3207	0.8602	0.4306	440	93	1.087	0.01426
			2nd	Mordred	LGBM	0.1322	0.3637	0.3293	0.8465	6.149	130	2.945	0.01665	
			3rd	Mol2Vec	RF	0.1403	0.3745	0.3392	0.8403	3.243	11	150	43.55	0.5061
	NLPD	1st	Mordred	GP	0.1254	0.3542	0.3207	0.8602	0.4306	440	93	1.087	0.01426	1.087
		2nd	Mordred	GP (C)	0.139	0.3728	0.3376	0.8457	0.4765	440	88	0.8704	0.02548	
		3rd	Mol2Vec	GP	0.1444	0.3801	0.3442	0.845	0.5331	11	66	0.9326	0.008236	
clearance	ADME(T)	NRMSE	1st	Mol2Vec	GP	1.05	1.025	0.4472	0.5638	1.459	19	76	0.8304	0.008322
			2nd	ChemBERTa-2	LGBM	1.053	1.026	0.4478	0.5702	3.728	7	55	4.251	0.0441
			3rd	ChemBERTa-2	GP	1.064	1.032	0.4502	0.5596	1.45	7	66	1.207	0.008383
	NLPD	1st	ChemBERTa-2	GP	1.064	1.032	0.4502	0.5596	1.45	7	66	1.207	0.008383	1.207
		2nd	Mol2Vec	GP	1.05	1.025	0.4472	0.5638	1.459	19	76	0.8304	0.008322	
		3rd	ChemBERTa-2	GP (C)	1.075	1.037	0.4525	0.5515	1.462	7	67	2.595	0.01472	
clearance_hepatocyte_az	ADME(T)	NRMSE	1st	Mordred	LGBM	1.991	44.62	0.7315	0.4169	7.77	470	180	23.27	0.0728
			2nd	ChemBERTa-2	GP	2005	44.77	0.734	0.4115	5.219	8.1	59	1.867	0.008714
			3rd	ChemBERTa-2	RF	2044	45.21	0.7411	0.4029	7.679	8.1	310	44.62	0.3051
	NLPD	1st	MTL-BERT	GP (C)	2121	46.05	0.7549	0.3873	5.205	20	64	2.461	0.01341	
		2nd	MTL-BERT	GP	2157	46.44	0.7613	0.3749	5.209	20	73	1.804	0.008395	
		3rd	ChemBERTa-2	GP	2005	44.77	0.734	0.4115	5.219	8.1	59	1.867	0.008714	
clearance_microsome_az*	ADME(T)	NRMSE	1st	ECFP	KNN	1.115	1.056	0.4295	0.6162	-	0.4	0.88	0.04638	0.03608
			2nd	MTL-BERT	GP	1.157	1.076	0.4415	0.611	1.469	14	76	1.726	0.008289
			3rd	Graph	GNN	1.177	1.085	0.4453	0.6023	1.539	12	160	196.6	0.657
	NLPD	1st	MTL-BERT	GP (C)	1.105	1.051	0.4315	0.6222	1.44	14	69	3.035	0.01416	
		2nd	ChemBERTa-2	GP (C)	1.111	1.054	0.4328	0.6205	1.464	7.3	65	0.8918	0.01536	
		3rd	MTL-BERT	GP	1.157	1.076	0.4415	0.611	1.469	14	76	1.726	0.008289	
esol	ADME(T)	NRMSE	1st	Mordred	LGBM	0.1262	0.3553	0.2692	0.9385	4.002	240	180	14.26	0.06709
			2nd	Mordred	SVM	0.1401	0.3743	0.2836	0.931	0.5157	240	55	1.422	0.8755
			3rd	Mordred	RF	0.1454	0.3814	0.2889	0.9292	4.549	240	670	98.49	0.3131
	NLPD	1st	ChemBERTa-2	GP (C)	0.2061	0.454	0.2988	0.9019	0.5575	8.2	96	3.14	0.01525	
		2nd	Mordred	GP	0.1556	0.3945	0.2988	0.9238	0.5618	240	120	4.061	0.01754	
		3rd	Mol2Vec	GP (C)	0.191	0.4371	0.3311	0.9049	0.565	12	85	3.746	0.01534	
freesolv	ADME(T)	NRMSE	1st	Mordred	LGBM	0.3928	0.6267	0.4856	0.8325	33.49	87	75	0.6068	0.009464
			2nd	Graph	GNN	0.3966	0.6298	0.4885	0.874	4.126	1.7	130	60.12	0.3792

Dataset	Property Class	Best By	Rank	Descriptor	Model	MSE	RMSE	NRMSE	Pearson R	NLPD	Featurisation (s)	Hyperparameter Optimisation (s)	Training (s)	Inference (s)	
half_life_obach*	ADME(T)	NRMSE	3rd	ChemBERTa-2	MLP	0.4251	0.652	0.5052	0.8436	2.291	3.7	9	0.9642	0.005376	
			1st	Graph	GNN (C)	0.4126	0.6423	0.4983	0.8705	0.6894	0.894	1.7	560	194.4	2.282
			2nd	Mordred	GP	0.476	0.6899	0.5346	0.8324	0.9408	0.832	87	70	0.832	0.01183
	ADME(T)	NRMSE	3rd	Mordred	SVM (C)	0.7053	0.8398	0.6507	0.8107	1.033	85	62	0.7094	0.9062	
			1st	Mordred	GP	1.108	1.052	0.5636	0.5671	1.481	350	61	0.8566	0.01273	
			2nd	Mordred	KNN	1.115	1.056	0.5655	0.5548	1.10.6	350	1.4	0.8094	0.02876	
	ADME(T)	NRMSE	3rd	Mordred	LGBM	1.122	1.059	0.5673	0.5563	4.388	350	100	100	2.125	0.0142
			1st	Mordred	GP	1.108	1.052	0.5636	0.5671	1.481	350	61	0.8566	0.01273	
			2nd	ChemBERTa-2	GP	1.18	1.086	0.5817	0.5246	1.49	5.7	65	0.7591	0.0104	
ld50_zhu	ADME(T)	NRMSE	3rd	Mol2Vec	GP	1.181	1.087	0.582	0.5377	1.493	4	62	2.453	0.008268	
			1st	Graph	GNN	0.6899	0.8306	0.728	0.6462	6.24	14	1100	1310	5.283	
			2nd	Mol2Vec	LGBM	0.7406	0.8606	0.7542	0.6084	23.46	20	260	9.157	0.2473	
	ADME(T)	NRMSE	3rd	Graph	GNN	0.7463	0.8639	0.7571	0.6067	1.764	35	960	361.3	4.465	
			1st	Mordred	GP	0.7953	0.8918	0.7816	0.5683	1.208	1700	1000	12.63	0.1296	
			2nd	ChemBERTa-2	GP	0.7545	0.8686	0.7613	0.5903	1.237	36	800	12.24	0.03781	
	ADME(T)	NRMSE	3rd	Mol2Vec	GP	0.7567	0.8699	0.7624	0.5962	1.253	20	830	40.28	0.03379	
			1st	Graph	GNN	0.416	0.645	0.3794	0.843	1.288	11	760	448.9	3.53	
			2nd	Graph	GNN	0.4624	0.68	0.4	0.8219	1.034	42	560	675.6	2.487	
ppbr_az*	ADME(T)	NRMSE	3rd	Mordred	LGBM	0.492	0.7014	0.4126	0.8142	5.341	1800	620	14.63	0.115	
			1st	Mol2Vec	GP	0.5409	0.7354	0.4326	0.7868	1.163	13	550	5.141	0.02227	
			2nd	MTL-BERT	GP	0.6037	0.777	0.457	0.7755	1.175	15	380	13.52	0.01613	
	ADME(T)	NRMSE	3rd	ChemBERTa-2	GP	0.5814	0.7625	0.4485	0.7699	1.19	26	580	5.879	0.02426	
			1st	Mordred	LGBM	0.0362	0.1903	1.072	0.5731	12.3	840	320	2.592	0.02986	
			2nd	Mol2Vec	MLP	0.03713	0.1927	1.086	0.5349	3.487	13	9.9	1.511	0.0137	
	ADME(T)	NRMSE	3rd	Mol2Vec	SVM	0.03745	0.1935	1.09	0.531	2.784	13	29	0.7714	0.5016	
			1st	ChemBERTa-2	MLP (C)	0.03968	0.1992	1.122	0.4877	-0.461	13	75	8.423	0.1147	
			2nd	Mol2Vec	LGBM (C)	0.03918	0.1979	1.115	0.493	-0.4526	13	270	5.501	0.1399	
vdss_lombardo*	ADME(T)	NRMSE	3rd	Mordred	RF (C)	0.03833	0.1958	1.103	0.5108	-0.4249	840	6800	2089	6.193	
			1st	Mordred	GP	0.8723	0.934	0.3999	0.7131	1.391	620	79	2.132	0.01709	
			2nd	Mordred	RF	0.8769	0.9364	0.401	0.7143	1.601	620	730	54.87	0.2139	
	ADME(T)	NRMSE	3rd	Mordred	LGBM	0.8817	0.939	0.4021	0.7087	2.201	620	200	15.42	0.07121	
			1st	Mordred	GP (C)	0.8709	0.9332	0.3996	0.7084	1.388	620	74	1.164	0.029	
			2nd	Mordred	GP	0.8723	0.934	0.3999	0.7131	1.391	620	79	2.132	0.01709	
	ADME(T)	NRMSE	3rd	MTL-BERT	GP (C)	1.011	1.005	0.4305	0.6506	1.441	21	65	0.8986	0.1015	
			1st	Mordred	LGBM	0.5307	0.7285	0.5057	0.8615	4.806	820	320	18.48	0.1015	
			2nd	Mol2Vec	LGBM	0.5469	0.7395	0.5134	0.8568	4.389	13	84	4.67	0.08656	
ADME(T)	NRMSE	3rd	Mol2Vec	RF	0.5507	0.7421	0.5152	0.8653	5.64	13	330	98.47	0.5071		
		1st	Mol2Vec	GP (C)	0.5119	0.7155	0.4967	0.8669	1.082	13	96	2.04	0.01539		
		2nd	Mol2Vec	GP	0.5513	0.7425	0.5154	0.8628	1.09	13	170	2.399	0.01026		
ADME(T)	NRMSE	3rd	ECFP	GP	0.6245	0.7903	0.556	0.8442	1.156	0.58	160	1.868	0.00819		
		1st	Mordred	RF	0.4051	0.6365	0.2456	0.8978	1.203	370	460	136	0.5117		
		2nd	ECFP	GP	0.4206	0.6485	0.252	0.8925	0.9754	0.28	68	2.507	0.007291		
ADME(T)	NRMSE	3rd	Mordred	GP	0.4458	0.6677	0.2577	0.8849	1.021	370	71	1.356	0.01312		
		1st	ECFP	GP	0.4206	0.6485	0.252	0.8925	0.9754	0.28	68	2.507	0.007291		
		2nd	Mordred	GP	0.4458	0.6677	0.2577	0.8849	1.021	370	71	1.356	0.01312		
ADME(T)	NRMSE	3rd	Mordred	GP (C)	0.4734	0.688	0.2655	0.8759	1.029	370	52	1.026	0.02303		

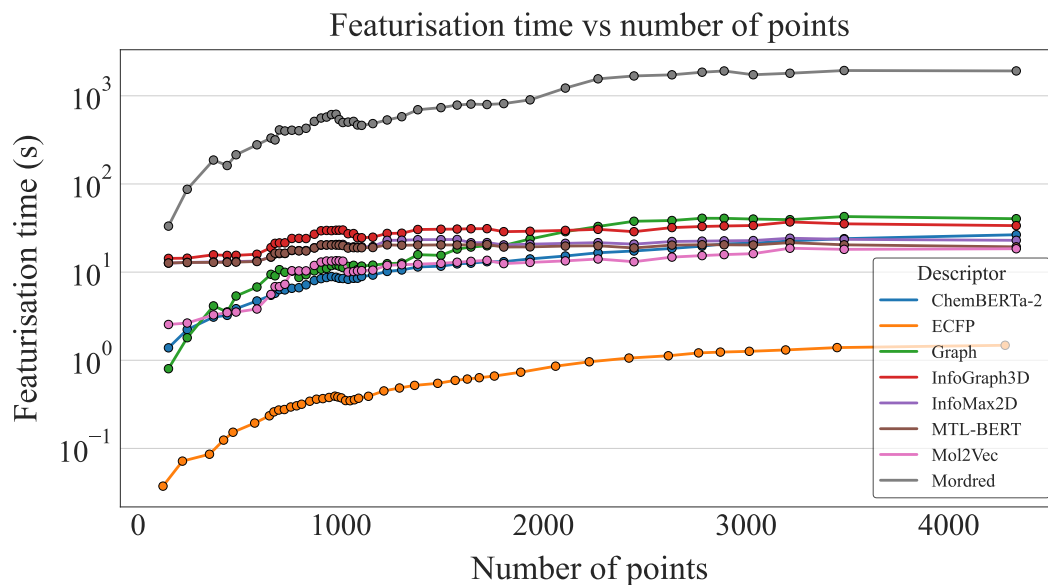
Dataset	Property Class	Best By	Rank	Descriptor	Model	MSE	RMSE	NRMSE	Pearson R	NLPD	Featurisation (s)	Hyperparameter Optimisation (s)	Training (s)	Inference (s)
CHEMBL1871_Ki	QSAR	NRMSE	1st	ECFP	GP	0.4178	0.6464	0.3778	0.7718	1.026	0.27	67	1.226	0.009734
			2nd	Graph	GNN	0.431	0.6565	0.3806	0.7639	1.035	2	130	110.4	0.6127
			3rd	ChemBERTa-2	GP	0.4526	0.6727	0.39	0.7511	0.985	6.3	69	2.775	0.007935
	NLPD	1st	ChemBERTa-2	GP	0.4526	0.6727	0.39	0.7511	0.985	6.3	69	2.775	0.007935	0.007935
		2nd	ChemBERTa-2	GP (C)	0.4636	0.6809	0.3947	0.7518	0.9972	6.3	67	1.254	0.009734	0.01374
		3rd	ECFP	GP	0.4178	0.6464	0.3778	0.7718	1.026	0.27	67	1.226	0.009734	0.009734
CHEMBL2034_Ki	QSAR	NRMSE	1st	ECFP	MLP	0.4397	0.6631	0.4382	0.7729	2.761	0.3	11	1.621	0.007341
			2nd	ChemBERTa-2	GP	0.4591	0.6776	0.4478	0.7639	1.004	6.5	74	2.489	0.007646
			3rd	ECFP	GP	0.4768	0.6905	0.4563	0.7523	1.033	0.3	75	0.7797	0.009248
	NLPD	1st	ChemBERTa-2	GP	0.4591	0.6776	0.4478	0.7639	1.004	6.5	74	2.489	0.007646	0.007646
		2nd	ECFP	GP	0.4768	0.6905	0.4563	0.7523	1.033	0.3	75	0.7797	0.009248	0.009248
		3rd	MTL-BERT	GP	0.5161	0.7184	0.4748	0.7287	1.045	1.3	71	2.941	0.007719	
CHEMBL2047_EC50	QSAR	NRMSE	1st	Mol2Vec	GP	0.3511	0.5925	0.4229	0.7995	0.8519	4.5	67	2.041	0.007755
			2nd	Mol2Vec	SVM	0.3552	0.596	0.4253	0.7995	1.114	4.5	4.5	0.111	0.07414
			3rd	ECFP	GP	0.3596	0.5997	0.4279	0.7923	0.8474	0.24	65	2.19	0.00704
	NLPD	1st	ECFP	GP	0.3596	0.5997	0.4279	0.7923	0.8474	0.24	65	2.19	0.00704	0.00704
		2nd	Mol2Vec	GP	0.3511	0.5925	0.4229	0.7995	0.8519	4.5	67	2.041	0.007755	0.007755
		3rd	Mordred	GP	0.4321	0.6574	0.4691	0.7451	0.8723	3.90	62	2.35	0.0116	
CHEMBL204_Ki	QSAR	NRMSE	1st	ECFP	GP	0.4836	0.6954	0.2982	0.895	1.145	1.2	200	17.56	0.0136
			2nd	Mordred	GP	0.3886	0.7672	0.3287	0.8692	1.256	14.00	250	5.271	0.03871
			3rd	Mol2Vec	GP	0.5906	0.7685	0.3293	0.868	1.238	9.8	230	17.82	0.01218
	NLPD	1st	ECFP	GP (C)	0.5126	0.716	0.307	0.8869	1.073	1.2	170	10.64	0.02251	
		2nd	ECFP	GP	0.4836	0.6954	0.2982	0.895	1.145	1.2	200	17.56	0.0136	
		3rd	Mol2Vec	GP	0.5906	0.7685	0.3293	0.868	1.238	9.8	230	17.82	0.01218	
CHEMBL2147_Ki	QSAR	NRMSE	1st	ECFP	GP (C)	0.6697	0.8183	0.3507	0.8487	1.202	9.8	170	10.64	0.02251
			2nd	ECFP	GP	0.3647	0.6039	0.1589	0.9465	0.9583	0.53	110	1.984	0.008692
			3rd	ECFP	SVM	0.3801	0.6165	0.1622	0.9442	1.288	0.53	41	1.082	0.7604
	NLPD	1st	Mol2Vec	GP	0.4746	0.6889	0.1812	0.9294	1.077	1.2	100	7.693	0.008855	
		2nd	ECFP	GP (C)	0.3843	0.62	0.1631	0.9434	0.9539	0.53	95	1.776	0.01422	
		3rd	ECFP	GP	0.3647	0.6039	0.1589	0.9465	0.9583	0.53	110	1.984	0.008692	
CHEMBL214_Ki	QSAR	NRMSE	1st	Mol2Vec	GP	0.4746	0.6889	0.1812	0.9294	1.077	1.2	100	7.693	0.008855
			2nd	ECFP	GP	0.4661	0.6827	0.4209	0.8123	3.156	1.3	240	7.296	5.337
			3rd	ECFP	KNN	0.5245	0.7242	0.4465	0.7854	-	4.9	0.3149	0.3095	
	NLPD	1st	ECFP	GP (C)	0.486	0.6971	0.4298	0.804	1.044	1.3	180	11.3	0.02666	
		2nd	ECFP	GP	0.4634	0.6808	0.4197	0.8141	1.052	1.3	210	12.76	0.01651	
		3rd	Mol2Vec	GP	0.5408	0.7354	0.4536	0.7803	1.127	1.3	290	14.34	0.01541	
CHEMBL218_EC50	QSAR	NRMSE	1st	ECFP	RF	0.4648	0.6818	0.4317	0.7469	2.806	0.39	78	5.195	0.205
			2nd	ECFP	GP	0.467	0.6834	0.4327	0.7516	1.052	0.39	81	2.219	0.007888
			3rd	ECFP	SVM	0.4884	0.6989	0.4425	0.7422	9.158	0.39	23	0.6373	0.4479
	NLPD	1st	ECFP	GP (C)	0.4547	0.6743	0.427	0.7571	1.004	0.39	72	0.9433	0.0134	
		2nd	ECFP	GP	0.467	0.6834	0.4327	0.7516	1.052	0.39	81	2.219	0.007888	
		3rd	Mol2Vec	GP (C)	0.5035	0.7095	0.451	0.7272	1.057	1.2	69	3.053	0.0153	
CHEMBL219_Ki	QSAR	NRMSE	1st	ECFP	GP	0.5281	0.7267	0.4664	0.7596	1.115	0.72	150	2.705	0.01147
			2nd	ECFP	SVM	0.5534	0.7439	0.4774	0.7474	3.979	0.72	75	2.09	1.47
			3rd	Mordred	GP	0.5676	0.7534	0.4839	0.7409	1.151	810	3.048	0.02661	
	NLPD	1st	ECFP	GP	0.5281	0.7267	0.4664	0.7596	1.115	0.72	150	2.705	0.01147	

Dataset	Property Class	Best By	Rank	Descriptor	Model	MSE	RMSE	NRMSE	Pearson R	NLPD	Featurisation (s)	Hyperparameter Optimisation (s)	Training (s)	Inference (s)	
CHEMBL228_Ki	QSAR	NRMSE	2nd	Mordred	GP (C)	0.5676	0.7534	0.4839	0.7409	1.151	810	170	3.048	0.02661	
			3rd	ECFP	GP (C)	0.622	0.7887	0.5062	0.7097	1.162	0.72	93	160	4.673	0.01696
			1st	ECFP	GP	0.4758	0.6898	0.3731	0.823	1.072	0.61	160	6	6	0.009946
			2nd	Mol2Vec	GP	0.5387	0.734	0.3981	0.7987	1.155	1.3	160	120	17.2	0.01028
			3rd	ECFP	RF	0.5474	0.7398	0.4001	0.7942	2.24	0.61	98	6	6	0.009946
			3rd	ECFP	GP (C)	0.5211	0.7218	0.3904	0.8044	1.067	0.61	160	84	2.077	0.01787
CHEMBL231_Ki	QSAR	NRMSE	2nd	ECFP	GP (C)	0.4758	0.6898	0.3731	0.823	1.072	0.61	76	1.041	0.008533	
			3rd	Mol2Vec	GP (C)	0.5417	0.736	0.3993	0.7965	1.086	1.3	70	1.313	0.01502	
			1st	Mol2Vec	GP	0.436	0.6603	0.3503	0.8589	0.9176	21	460	0.992	0.732	
			2nd	Mordred	GP	0.4395	0.6629	0.3517	0.8561	1.083	460	38	1.041	0.008533	
			3rd	Mordred	SVM	0.4602	0.6784	0.36	0.8486	9.198	460	67	0.992	0.732	
			2nd	Mol2Vec	GP (C)	0.436	0.6603	0.3503	0.8589	0.9176	21	76	1.041	0.008533	
CHEMBL233_Ki	QSAR	NRMSE	1st	ECFP	GP	0.4933	0.7024	0.3727	0.8371	0.9817	21	200	5.009	0.01877	
			2nd	Mol2Vec	GP (C)	0.4638	0.681	0.3611	0.85	0.9889	0.37	85	5.009	0.01877	
			3rd	ECFP	GP	0.532	0.7294	0.3821	0.8318	1.131	1.4	210	5.801	4.101	
			2nd	ECFP	SVM	0.545	0.7382	0.3867	0.8278	2.929	1.4	270	25.33	0.04264	
			3rd	Mordred	GP	0.5694	0.7546	0.395	0.8237	1.148	2700	180	6.779	0.02466	
			1st	ECFP	GP (C)	0.5448	0.7381	0.3866	0.8283	1.106	1.4	200	5.009	0.01877	
CHEMBL234_Ki	QSAR	NRMSE	2nd	ECFP	GP	0.532	0.7294	0.3821	0.8318	1.131	1.4	230	15.89	0.01801	
			3rd	ECFP	GP (C)	0.6013	0.7755	0.4059	0.8103	1.147	25	180	4.336	0.02798	
			1st	ChemBERTa-2	GP (C)	0.3897	0.6242	0.3435	0.8483	0.9961	1.4	230	15.89	0.01801	
			2nd	ECFP	SVM	0.402	0.6341	0.3489	0.8424	2.803	1.4	290	7.862	5.633	
			3rd	ECFP	RF	0.4228	0.6502	0.3578	0.8361	2.237	1.4	280	38.87	0.4115	
			1st	ECFP	GP (C)	0.4132	0.6428	0.3537	0.8381	0.9644	1.4	190	5.264	0.03667	
CHEMBL235_EC50	QSAR	NRMSE	2nd	ECFP	GP	0.3897	0.6242	0.3435	0.8483	0.9961	1.4	350	30.31	0.05043	
			3rd	Mordred	GP	0.4679	0.684	0.3776	0.8176	1.052	1800	170	47.49	0.6094	
			1st	ECFP	RF	0.4053	0.6366	0.4051	0.7989	2.462	0.96	150	2.417	0.01927	
			2nd	Mol2Vec	GP	0.4196	0.6477	0.4122	0.7929	1.065	15	170	2.315	0.01216	
			3rd	Mordred	LGBM	0.421	0.6489	0.4129	0.7909	1.845	1200	410	21.98	0.1559	
			1st	ECFP	GP (C)	0.4368	0.6609	0.4206	0.7835	0.9952	0.96	160	2.965	0.01352	
CHEMBL236_Ki	QSAR	NRMSE	2nd	Mol2Vec	GP (C)	0.4607	0.6788	0.4319	0.7714	1.037	1.3	170	3.426	0.01242	
			3rd	ECFP	GP	0.4245	0.6515	0.4146	0.7907	1.038	0.96	160	3.451	0.01242	
			1st	ECFP	GP	0.4497	0.6706	0.3266	0.8657	1.053	1.3	170	2.389	2.389	
			2nd	ECFP	SVM	0.4825	0.6946	0.3383	0.8566	2.815	1.3	130	23.62	0.4084	
			3rd	ECFP	RF	0.5307	0.7285	0.3548	0.8383	2.134	1.3	170	3.451	0.01242	
			1st	ECFP	GP	0.4497	0.6706	0.3266	0.8657	1.053	1.3	150	2.275	0.02028	
CHEMBL237_EC50	QSAR	NRMSE	2nd	Mol2Vec	GP (C)	0.5206	0.7215	0.3514	0.845	1.093	1.3	140	2.459	0.01866	
			3rd	ECFP	GP (C)	0.5643	0.7512	0.3658	0.8281	1.135	16	73	0.8847	0.008166	
			1st	ECFP	GP	0.5692	0.7545	0.3754	0.8526	1.13	0.43	73	0.8847	0.008166	
			2nd	Mordred	GP	0.5802	0.7617	0.379	0.8471	1.235	980	83	1.202	0.01589	
			3rd	Mol2Vec	GP	0.5914	0.769	0.3826	0.8445	1.156	12	69	0.9364	0.00907	
			1st	ECFP	GP	0.5692	0.7545	0.3754	0.8526	1.13	0.43	73	0.8847	0.008166	
CHEMBL237_Ki	QSAR	NRMSE	2nd	Mol2Vec	GP (C)	0.5874	0.7664	0.3813	0.8433	1.165	0.43	70	0.9364	0.00907	
			3rd	ECFP	GP	0.4971	0.705	0.349	0.8548	1.079	1.2	180	13.17	0.01585	
			1st	ECFP	GP	0.5107	0.7146	0.3536	0.8483	1.158	17	4.304	0.01197		
			2nd	Mol2Vec	GP										

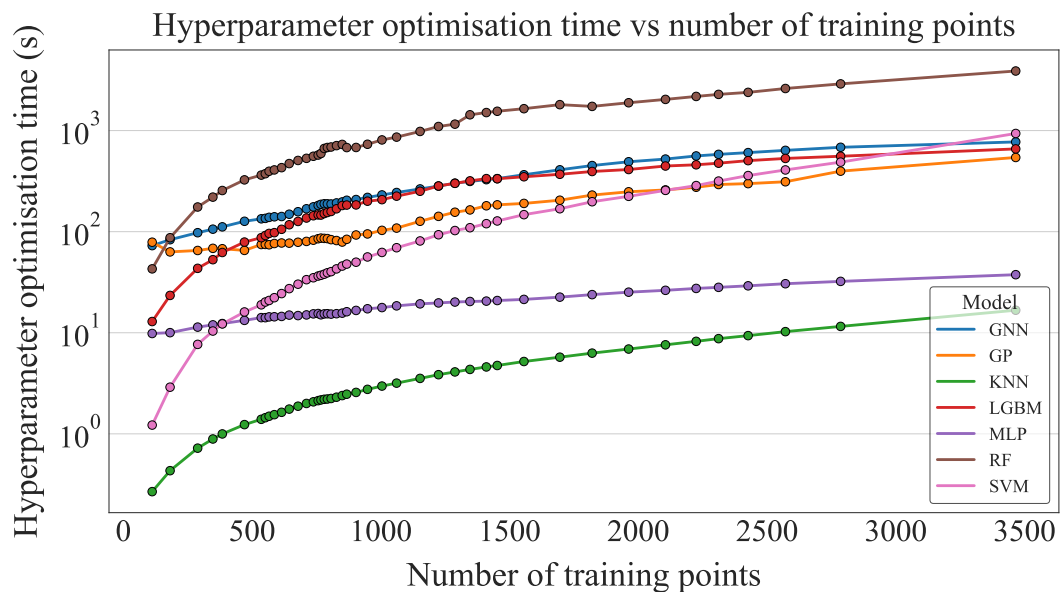
Dataset	Property Class	Best By	Rank	Descriptor	Model	MSE	RMSE	NRMSE	Pearson R	NLPD	Featurisation (s)	Hyperparameter Optimisation (s)	Training (s)	Inference (s)
CHEMBL238_Ki	QSAR	NRMSE	3rd	Mol2Vec	SVM	0.5148	0.7175	0.355	0.847	2.289	17	70	1.861	1.219
			1st	ECFP	GP	0.4971	0.705	0.349	0.8548	1.079	1.2	180	13.17	0.01585
			2nd	ECFP	GP (C)	0.5352	0.7316	0.3622	0.8416	1.091	1.2	160	7.686	0.02508
			3rd	Mol2Vec	GP (C)	0.5557	0.7455	0.3689	0.8338	1.122	17	180	2.893	0.02093
			1st	ECFP	RF	0.3802	0.6166	0.3426	0.8516	2.33	0.33	72	10.17	0.3049
			2nd	ECFP	GP	0.3848	0.6204	0.3447	0.8439	0.9647	0.33	77	4.395	0.006928
			3rd	ECFP	SVM	0.4035	0.6352	0.3529	0.8322	15.34	0.33	23	0.6411	0.4441
			1st	ECFP	GP (C)	0.3957	0.629	0.3495	0.8349	0.9404	0.33	65	0.8989	0.01275
			2nd	ECFP	GP	0.3848	0.6204	0.3447	0.8439	0.9647	0.33	77	4.395	0.006928
CHEMBL239_EC50	QSAR	NRMSE	3rd	Mol2Vec	GP (C)	0.453	0.6731	0.374	0.8078	0.9873	11	64	0.9135	0.01388
			1st	ECFP	GP	0.4454	0.6674	0.4252	0.8031	1.04	0.64	140	2.181	0.009566
			2nd	ECFP	SVM	0.4654	0.6822	0.4346	0.7957	3.161	0.64	67	1.864	1.342
			3rd	ECFP	RF	0.4898	0.6999	0.4459	0.7816	2.679	0.64	120	16.09	0.4087
			1st	ECFP	GP	0.4454	0.6674	0.4252	0.8031	1.04	0.64	140	2.181	0.009566
			2nd	ECFP	GP (C)	0.4943	0.703	0.4479	0.7787	1.056	0.64	82	2.008	0.0181
			3rd	Mol2Vec	GP (C)	0.5636	0.7507	0.4788	0.7508	1.11	13	82	1.817	0.01669
			1st	ECFP	GP	0.5338	0.7306	0.2653	0.9003	1.165	1.4	220	20.82	0.0155
			2nd	ECFP	KNN	0.5982	0.7734	0.2809	0.8876	-	4.3	220	0.2779	0.2756
CHEMBL244_Ki	QSAR	NRMSE	3rd	Mordred	GP	0.6181	0.7862	0.2845	0.8815	1.271	1800	190	6.09	0.0458
			1st	ECFP	GP (C)	0.5882	0.7669	0.2786	0.8875	1.139	1.4	290	2.851	0.03023
			2nd	ECFP	GP	0.5338	0.7306	0.2653	0.9003	1.165	1.4	220	20.82	0.0155
			3rd	Mordred	GP (C)	0.6349	0.7968	0.2883	0.8776	1.195	1800	260	3.298	0.08088
			1st	ECFP	GP	0.4815	0.6939	0.4337	0.7666	1.015	0.31	65	2.785	0.007548
			2nd	ECFP	RF	0.4892	0.6994	0.4371	0.7604	2.848	0.31	65	17.51	0.5062
			3rd	MTL-BERT	MLP	0.557	0.7463	0.4665	0.7305	4.579	20	8.1	1.538	0.006727
			1st	ECFP	GP	0.4815	0.6939	0.4337	0.7666	1.015	0.31	65	2.785	0.007548
			2nd	ECFP	GP (C)	0.5251	0.7246	0.4529	0.7438	1.056	0.31	61	2.433	0.01285
CHEMBL264_Ki	QSAR	NRMSE	3rd	Mol2Vec	GP	0.5599	0.7483	0.4677	0.7233	1.122	11	70	2.713	0.008332
			1st	ECFP	GP	0.3333	0.5773	0.3749	0.8423	0.9362	1	180	10.85	0.01314
			2nd	ECFP	SVM	0.3413	0.5842	0.3793	0.8384	2.228	1	160	5.476	3.475
			3rd	Mordred	LCBM	0.3819	0.618	0.4019	0.8229	1.062	1200	480	4.07	0.05529
			1st	ECFP	GP (C)	0.3677	0.6064	0.3938	0.8241	0.8929	1	150	6.061	0.02119
			2nd	ECFP	GP	0.3333	0.5773	0.3749	0.8423	0.9362	1	180	10.85	0.01314
			3rd	Mordred	GP (C)	0.4255	0.6523	0.4242	0.8038	0.9688	1200	180	14.33	0.06694
			1st	ChemBERTa-2	GP (C)	0.5531	0.7437	0.493	0.7517	1.108	9.5	85	5.995	0.009376
			2nd	Graph	GNN	0.5593	0.7479	0.4957	0.7492	1.566	3.3	230	167.8	1.089
CHEMBL287_Ki	QSAR	NRMSE	3rd	Mordred	GP	0.5602	0.7485	0.4961	0.7486	1.106	510	81	8.1	0.01978
			1st	Mordred	GP	0.5602	0.7485	0.4961	0.7486	1.106	510	81	2.441	0.01978
			2nd	ChemBERTa-2	GP	0.5531	0.7437	0.493	0.7517	1.108	9.5	85	5.995	0.009376
			3rd	ECFP	GP	0.5722	0.7564	0.5096	0.7426	1.129	0.43	84	4.557	0.00845
			1st	ECFP	GP	0.3601	0.6	0.2261	0.9051	0.812	0.41	91	2.213	0.007616
			2nd	ECFP	SVM	0.3717	0.6096	0.2298	0.9021	4.363	0.41	20	0.5046	0.3613
			3rd	Mol2Vec	GP	0.3867	0.6218	0.2346	0.8681	1.1	83	1.444	0.00857	
			1st	Mordred	GP	0.416	0.645	0.2433	0.8897	0.7827	570	99	2.019	0.01439
			2nd	ECFP	GP	0.3601	0.6	0.2261	0.9051	0.812	0.41	91	2.213	0.007616
CHEMBL2971_Ki	QSAR	NRMSE	3rd	Mol2Vec	GP	0.3867	0.6218	0.2346	0.8982	0.8681	11	83	1.444	0.00857

Dataset	Property Class	Best By	Rank	Descriptor	Model	MSE	RMSE	NRMSE	Pearson R	NLPD	Featurisation (s)	Hyperparameter Optimisation (s)	Training (s)	Inference (s)	
CHEMBL3979_EC50	QSAR	NRMSE	1st	Mordred	GP	0.4307	0.6563	0.3316	0.8097	0.9923	560	100	2.258	0.01871	
			2nd	ECFP	GP	0.4417	0.6646	0.3331	0.8048	0.9625	560	91	5.91	0.01027	
			3rd	Mordred	LCBM	0.4612	0.6791	0.3432	0.7944	3.581	0.925	560	190	15.02	0.07725
			1st	ECFP	GP (C)	0.45	0.6708	0.3362	0.8004	0.9344	0.47	77	77	2.81	0.01429
			2nd	ECFP	GP	0.4417	0.6646	0.3331	0.8048	0.9625	0.47	91	91	5.91	0.01027
			3rd	Mordred	GP	0.4307	0.6563	0.3316	0.8097	0.9923	560	100	2.258	0.01871	
CHEMBL4005_Ki	QSAR	NRMSE	1st	ECFP	GP	0.3057	0.5529	0.3581	0.8357	0.7863	0.38	79	2.837	0.007828	
			2nd	Mordred	GP	0.3526	0.5982	0.3845	0.8072	0.9172	600	88	1.057	0.01459	
			3rd	ECFP	RF	0.3579	0.5982	0.3874	0.8061	2.366	0.38	58	15.31	0.5058	
			1st	ECFP	GP	0.3057	0.5529	0.3581	0.8357	0.7863	0.38	79	2.837	0.007828	
			2nd	ECFP	GP (C)	0.3165	0.5626	0.3643	0.8278	0.8143	0.38	75	0.7651	0.01328	
			3rd	Mordred	GP	0.3526	0.5938	0.3845	0.8072	0.9172	600	88	1.057	0.01459	
CHEMBL4203_Ki	QSAR	NRMSE	1st	ECFP	GP	0.738	0.859	0.6136	0.6087	1.254	0.24	70	1.428	0.007531	
			2nd	ECFP	SVM	0.7739	0.8797	0.6284	0.5974	24.67	0.24	13	0.3622	0.2618	
			3rd	ECFP	LCBM	0.7743	0.8799	0.6285	0.5793	1.784	0.24	7.3	0.09864	0.006562	
			1st	ECFP	GP	0.738	0.859	0.6136	0.6087	1.254	0.24	70	1.428	0.007531	
			2nd	Mol2Vec	GP (C)	0.792	0.8899	0.6357	0.564	1.305	11	63	0.658	0.01401	
			3rd	ECFP	GP	0.7998	0.8943	0.6388	0.557	1.336	11	65	0.6155	0.007369	
CHEMBL4616_EC50	QSAR	NRMSE	1st	ECFP	GP	0.3477	0.5897	0.4315	0.7758	0.9058	0.31	62	2.055	0.007115	
			2nd	ChemBERTa-2	GP	0.3759	0.6131	0.4447	0.7565	0.9429	6.8	66	0.9749	0.006916	
			3rd	Mordred	GP	0.3805	0.6169	0.4315	0.7558	0.9058	0.31	53	0.7854	0.0123	
			1st	ECFP	GP	0.3477	0.5897	0.4315	0.7758	0.9058	0.31	62	2.055	0.007115	
			2nd	ECFP	GP (C)	0.3702	0.6084	0.4452	0.7581	0.94	0.31	53	2.074	0.01249	
			3rd	ChemBERTa-2	GP	0.3759	0.6131	0.4447	0.7565	0.9429	6.8	66	0.9749	0.006916	
CHEMBL4792_Ki	QSAR	NRMSE	1st	Mol2Vec	GP	0.439	0.6626	0.4225	0.7862	1.101	13	99	2.242	0.009576	
			2nd	ECFP	GP	0.4493	0.6703	0.4274	0.7812	1.019	0.58	110	6.676	0.009815	
			3rd	ECFP	SVM	0.457	0.676	0.4311	0.78	15.73	0.58	48	1.35	0.9447	
			1st	ECFP	GP	0.4493	0.6703	0.4274	0.7812	1.019	0.58	94	6.452	0.01603	
			2nd	ECFP	GP (C)	0.4817	0.694	0.4426	0.76	1.042	0.58	94	6.452	0.01603	
			3rd	Mol2Vec	GP (C)	0.4669	0.6833	0.4357	0.7712	1.049	13	86	2.136	0.01659	
COVID_moonshot*	QSAR	NRMSE	1st	Mol2Vec	LCBM	2.404	1.55	0.3239	0.5568	1.977	7.7	91	4.981	0.1105	
			2nd	Mordred	GP	2.405	1.551	0.324	0.5523	1.883	920	2.99	0.02704		
			3rd	Mordred	GP	2.424	1.557	0.3252	0.5489	1.958	920	20.44	0.1297		
			1st	ECFP	GP (C)	2.411	1.553	0.3244	0.5452	1.846	7.7	170	2.106	0.01869	
			2nd	ECFP	GP (C)	2.421	1.556	0.3354	0.5293	1.852	0.69	100	2.207	0.01658	
			3rd	Mordred	GP (C)	2.427	1.558	0.3254	0.5435	1.86	920	120	2.325	0.04902	
US9908845B2*	QSAR	NRMSE	1st	InfoMax2D	GP	4.372	2.091	0.4915	0.4728	2.173	13	45	1.034	0.005047	
			2nd	Mol2Vec	GP	4.431	2.105	0.4948	0.4847	2.158	2.7	47	0.7807	0.005049	
			3rd	ECFP	GP	4.418	2.102	0.5026	0.5059	2.263	0.11	44	1.813	0.005231	
			1st	InfoMax2D	GP	4.431	2.105	0.4948	0.4847	2.158	2.7	47	0.7807	0.005049	
			2nd	InfoMax2D	GP (C)	4.336	2.082	0.4894	0.477	2.16	13	51	0.4042	0.008049	
			3rd	InfoMax2D	GP	4.372	2.091	0.4915	0.4728	2.173	13	45	1.034	0.005047	

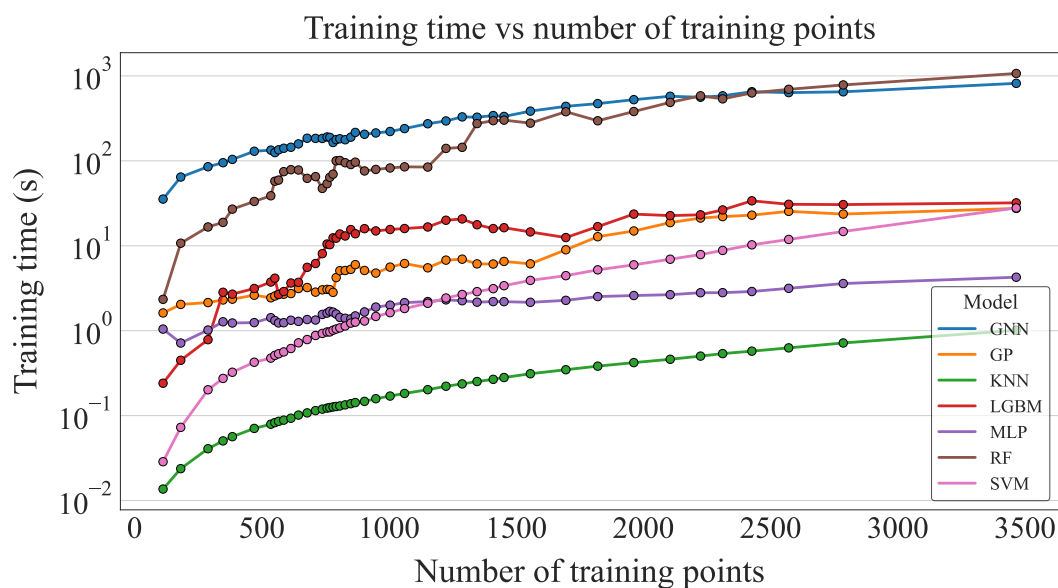
A.3 Runtime Measurements



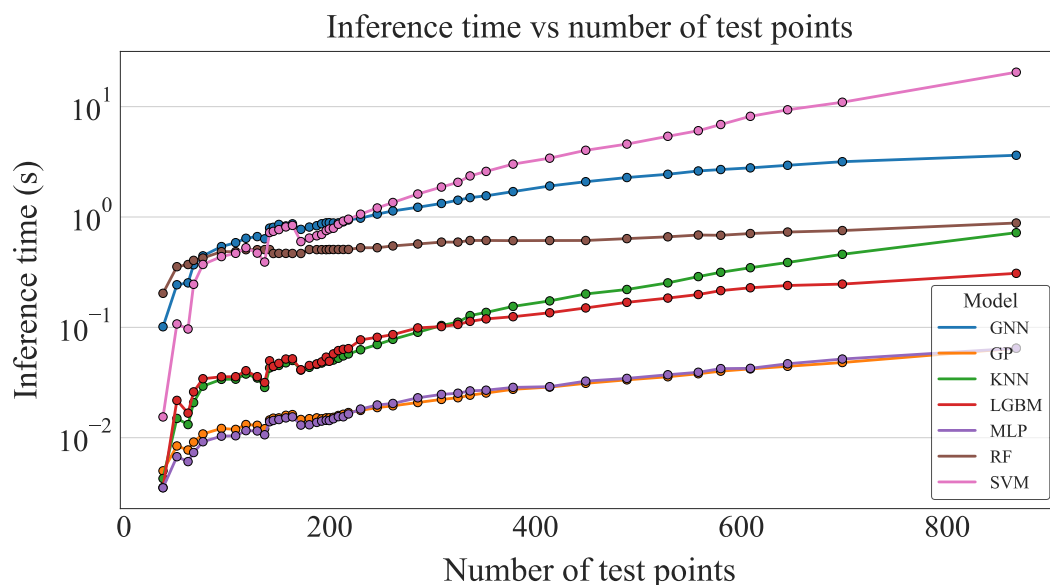
(a)



(b)



(c)



(d)

Figure A.1: Featurisation, hyperparameter optimisation, training and inference runtimes for single uncalibrated models by number of input points, split by descriptor (a) or model, (b), (c), (d). For (b), (c) and (d), points represent the maximum training time across all descriptors. In all cases, a rolling mean with window size 5 is applied point-wise for smoothing. The following descriptors were calculated on GPU: ChemBERTa-2, MTL-BERT, InfoMax2D, InfoGraph3D and the remainder on CPU. The following models were trained on GPU: Graph, GP, MLP. Remaining models were trained on CPU, with LGBM and RF trained using multiprocessing over 4 cores. The GPU used was an Nvidia T4.

A.4 Hyperparameter Optimisation Search Spaces

Table A.3: Hyperparameter search spaces by model. In the case of ensemble models, the same hyperparameters were used for all members. A random search was applied using a search space size of 20 and 3-fold cross validation for each hyperparameter combination. The final model was retrained with the optimal parameters on the whole training dataset.

Model	Hyperparameter	Search Values
SVM	C	1, 10, 100, 1000
	epsilon	0.1
	gamma	1.0e-06, 1.0e-05, 0.0001, 0.001, 0.01, 0.1
	kernel	RBF
RF	n_estimators	100, 250, 500, 1000
GP	kernel	RBF, Matern, RQ, Tanimoto
	n_iter	10, 100, 1000
	lr	0.01, 0.1, 1
LGBM	n_estimators	100, 200, 500, 1000
	max_depth	3, 4, 5, 6, 7
	learning_rate	0.01, 0.05, 0.1, 0.2, 0.3
	subsample	0.4, 0.45, 0.5, 0.55, 0.6, 0.65
	colsample_bytree	0.5, 0.6, 0.7, 0.8, 0.9, 1.0
	reg_alpha	0, 0.1, 1, 5, 10
	reg_lambda	0.1, 1, 10, 100
	min_child_weight	1, 3, 5
	num_leaves	10, 20, 40, 80, 200, 500
	min_child_samples	5, 10, 20, 40, 100
	tree_learner	feature
KNN	n_neighbors	3, 5, 11, 21
	weights	uniform, distance
MLP	batch_size	128, 256, 512
	learning_rate	0.0001, 0.0005, 0.001
	mlp_dropout	0.0, 0.1, 0.2, 0.3, 0.4, 0.5
	mlp_hidden	128, 256, 512, 1024
	mlp_n_layers	2, 3, 4
A-FP	batch_size	128, 256, 512
	learning_rate	1e-5, 0.0001, 0.001
	dropout	0.0, 0.1, 0.2, 0.3, 0.4, 0.5
GAT	batch_size	128, 256, 512
	learning_rate	1e-5, 0.0001, 0.001
	dropout	0.0, 0.1, 0.2, 0.3, 0.4, 0.5
GCN	batch_size	128, 256, 512
	learning_rate	0.0001, 0.0005, 0.001
	graph_conv_layers	16, 16, 32, 32, 64, 64
	batchnorm	True, False
	dropout	0.0, 0.2, 0.5
	predictor_dropout	0.0, 0.2, 0.5
DMPNN	batch_size	128, 256, 512
	learning_rate	1e-5, 0.0001, 0.001
	enc_dropout_p	0.00, 0.2, 0.5
	ff_dropout_p	0.00, 0.2, 0.5